Dynamic heat and mass transfer model
of an electric oven for energy analysis

Edgar Ramirez-Laboreo[a,*], Carlos Sagues[a], Sergio Llorente[b]

[a]*Departamento de Informática e Ingeniería de Sistemas (DIIS) and*
Instituto de Investigación en Ingeniería de Aragón (I3A),
Universidad de Zaragoza, Zaragoza 50018, Spain
[b]*Research and Development Department, Induction Technology, Product Division Cookers,*
BSH Home Appliances Group, Zaragoza 50016, Spain

Abstract

In this paper, a new heat and mass transfer model for an electric oven and the load placed inside is presented. The developed model is based on a linear lumped parameter structure that differentiates the main components of the appliance and the load, therefore reproducing the thermal dynamics of several elements of the system including the heaters or the interior of the product. Besides, an expression to estimate the water evaporation rate of the thermal load has been developed and integrated in the model so that heat and mass transfer phenomena are made interdependent. Simulations and experiments have been carried out for different cooking methods and the subsequent energy results, including energy and power time-dependent distributions, are presented. The very low computational needs of the model make it ideal for optimization processes involving a high number of simulations. This feature, together with the energy information also provided by the model, will permit the design of new ovens and control algorithms that may outperform the present ones in terms of energy efficiency.

Keywords: Electric oven, Thermal modeling, Lumped model, Energy analysis, Heat and mass transfer.

1. Introduction

Baking and roasting are generalized cooking methods consisting in heating the food inside an oven at a uniform temperature. In these processes, heat is transferred to the load mainly by means of radiation and convection. Although these are widely-known phenomena, complex and combined thermal, chemical, and mass transfer processes occur within the product and change its properties during the cooking. This complexity often requires the process to be supervised or even controlled by an 'expert', which usually leads to suboptimal and highly variable results in terms of food quality and energy consumption. It is then necessary to improve the understanding of the system dynamics in order to make progress in the automation and optimization of those cooking processes [1]. For this purpose, a complete model which includes both the load and the oven itself could provide a full overview of interest variables such as heat fluxes, thermal energy stored in the oven components or losses to the ambient. In short, this knowledge may permit the complete optimization of the process, achieving optimal food results and minimum power consumption.

Some previous works were focused on developing simple thermal models for ovens, primarily to use them in the design of temperature controllers. See, e.g., [2], where a black-box ARMAX model was used, and the works in [3] and [4], where basic principles were utilized to build models that described the temperature dynamics of an oven cavity. Although these models proved their usefulness, they did not consider the

---

*Corresponding author. Tel.: +34 976 762 472
Email addresses: `ramirlab@unizar.es` (Edgar Ramirez-Laboreo), `csagues@unizar.es` (Carlos Sagues),
`sergio.llorente@bshg.com` (Sergio Llorente)

complete thermal behavior of the system because they were exclusively interested in the cavity temperature. Furthermore, none of them made a distinction between food and oven, so they were unable to know the energy transferred to the load or the internal temperature of the product.

On the other hand, some researches have analyzed diverse types of ovens by means of accurate although time consuming CFD of FEM models. See, e.g., the work in [5] for predicting the air temperature in an industrial biscuit baking oven or the intensive research in bread baking in [6] or in the works by Khatir et al. in [7] and later papers. Some works obtained valuable results for transient responses [8, 9], but the high computational requirements of the CFD and FEM approaches make them unviable for processes involving a high number of simulations, e.g., sensitivity analyses of the model parameters or optimization of temperature controllers.

Other research groups oriented their studies to the load itself, obtaining precise models for specific combinations of load and heating mode. Just to name a few, see, e.g., the work in [10], where a model that predicted the heat transferred to a metallic load was obtained, or the models presented in [11], [12] or [13], which included both thermal diffusivity and mass transfer phenomena in cake baking or meat roasting processes. These models provided good results, but most of them also required long calculations (FEM) and were hardly adaptable to other loads or heating modes. Additionally, in spite of being based on theoretical equations, experimental data will always be necessary to evaluate heat transfer coefficients, which in essence can be considered similar to an identification process.

In a different context, buildings have been thermally modeled by means of lumped capacitance models [14, 15, 16] with apparently good results. This modeling method is based on a simplification of the heat transfer equations and consists in evaluating the thermal system as a discrete set of thermal capacitances and resistances. However, if the parameter set is unknown and therefore an identification process is needed, model identifiability must be studied to guarantee the physical sense of the proposed structure. This property was not studied in any of the cited works and, consequently, their corresponding models must only be used to obtain temperature-time evolutions and not for extracting energy information from the system. To the best knowledge of the authors, lumped capacitance structures have never been used to model ovens.

In this paper, a new model for an electric oven is presented and some energy analyses are carried out to evaluate the system performance. This model, which is based on a lumped capacitance structure but including the effect of water evaporation, has been built according to a method previously presented by the authors [17]. Model identifiability has been studied so that the physical meaning of the model is not questioned. The main contribution of this work is obtaining a model that (1) includes both the components of the appliance and the load in its interior, (2) is accurate for pure convective, pure radiative or mixed heating methods, (3) estimates the water evaporation in the surface of the load, (4) explains the energy exchanges between zones including losses to the ambient, (5) is easily adaptable to modifications in the oven or to different loads and (6) requires a very low computational effort.

2. Materials and methods

2.1. Oven, load and measurement equipment

The oven used in this research is a commercial Bosch brand wall oven including four resistive heating elements and a fan that improves the heat distribution. The internal cavity, which is made of a steel sheet and is internally enameled, has dimensions $482 \times 329 \times 387$ mm (width by height by depth). The location of the heating elements and the fan in the cavity is schematically presented in Fig. 1. A fiberglass thermal blanket surrounds all sides of the cavity except for the front, which is covered by a metal-framed multilayer glass door. The oven is completed with the required electronic components and metal sheets on the bottom, top, left, right and rear sides that protect the system and define the external structure.

The thermal load investigated is the ceramic test brick Hipor, Skamol brand, with dimensions $230 \times 114 \times 64$ mm, 920 grams weight and unknown thermal conductivity. The brick is highly porous and permits a water absorption of 1050 grams if it is immersed in a water bath for 8 hours. The result is an approximately 2 kilogram load that evaporates water when heated, simulating the drying process that every product experiments during its cooking. It was placed centered in the oven cavity at a height of 155 mm
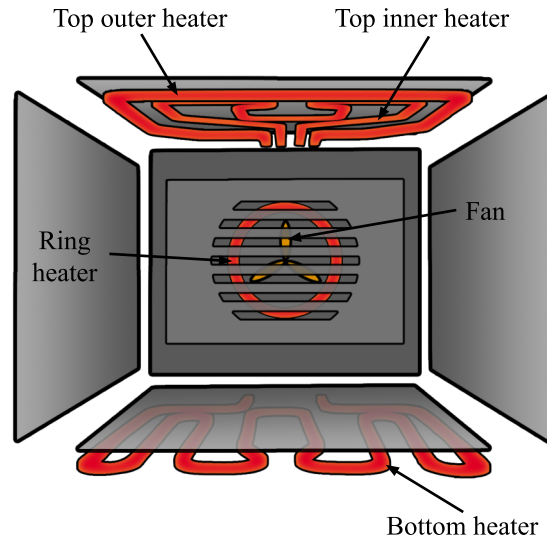
Fig. 1. Oven scheme. The model utilized in this research includes four heating elements (top outer, top inner, ring and bottom) and a fan that improves the heat distribution.
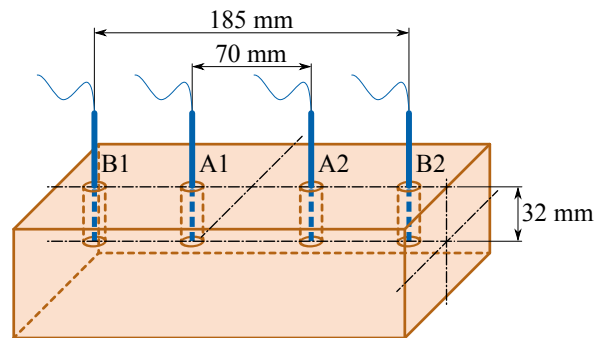

Fig. 2. Brick scheme with the location of the 1-mm-diameter drill holes. Four thermocouples (blue) measured the temperature in the base of the drill holes.

from the bottom. The utilization of this brick permitted the experiments to be highly reproducible, which is almost impossible if real food is used. Nevertheless, the modeling method is perfectly adaptable to different thermal loads since it only requires temperature, mass and power consumption measurements.

Both oven and load were prepared for the realization of experimental tests. One hundred and one type-K thermocouples were placed in different locations of the oven to measure the temperature in several points. Forty of them were homogeneously distributed on the oven cavity, forty-five on the external metal sheets and sixteen on the heating elements, four on each one. Besides, four 1-mm-diameter holes were drilled in the brick (Fig. 2) to insert thermocouples and measure internal temperatures. The experiments were conducted in a 20 m^2 air-conditioned laboratory whose temperature was stabilized to 23 ± 1°C. In order to record this temperature, an additional thermocouple was located in the middle of the laboratory.

Three Yokogawa Darwin DA100 data acquisition units connected to a personal computer permitted the temperature logging and recording, and a Yokogawa WT210 digital power meter recorded the total energy consumption. The oven grid was modified so that it was not placed in the lateral supports, but hung from a cable that went through a small drill hole in the top of the oven and which was connected to a KERN 440 weighing scales. This device permitted the brick mass to be measured and registered throughout the tests. The complete measurement line, including the sensors, the instruments and the computer, features

accuracies of $\pm 2^{o}$C in temperature, ± 0.02g in mass and ± 5W in power. Finally, a relay board specifically designed and activated by means of a National Instruments 9481 output module allowed the oven to be controlled by a computer where the selected algorithm was run.

2.2. Data recording methods

A common state at the beginning of a domestic cooking process is that the oven is at ambient temperature and the food has just been taken out of the refrigerator. To emulate this starting condition, the temperature of the oven at the beginning of the tests was 23 ± 1ºC, and the brick was at 5 ± 1ºC and water-saturated. Although this initial state was not really necessary for building the model, it improved the reproducibility of the experiments and allowed us to analyze the preheating stage, which is of particular interest because it requires a significant portion of the total energy consumption of the process.

The tests were divided in two different sets according to their main purpose. The first group (Set A) consisted of ten tests, with a duration of approximately 45 minutes, each using a different combination of heating elements, fan state (on/off) and set point temperature so that all possible heating modes were considered. The ceramic brick was consequently subjected to different cooking processes, including mixed and pure radiative and convective modes, in which the evaporated water and the internal temperature at the end of the tests changed considerably. During these tests, the mass of the thermal load and the temperatures given by the thermocouples were measured and logged.

Another set of longer experiments (Set B) was also carried out. Two three-hour tests were conducted in the oven, one with the fan activated and another deactivated, in which the heating elements were alternatively turned on so that only one of them was working at a time. The on/off cycles were determined by a hysteresis controller applied to the temperature of the center of the cavity. The hysteresis lower and upper bounds were respectively set to 150ºC and 250ºC since it is the usual operating range of the oven. This experiment design, in which the heating elements were activated separately, permitted the utilization of only one power measurement unit. Since the heating elements are nearly 100% efficient, the thermal power provided by each one was directly calculated as the total power consumption of the oven minus the power used by the fan and the light, which are known and equal to 25 W and 30 W, respectively. The power utilized by the electronics was considered negligible. The temperatures of all the thermocouples were also registered during these tests.

3. Modeling and identification

3.1. Thermal model

The model developed in this research is based on a linear lumped capacitance structure. Although this modeling method greatly simplifies the heat transfer differential equations, it provides a good enough approach to estimate the main temperatures of the system. Besides, if model identifiability is demonstrated, which means that there only exists a global optimum parameter set, it can even be used to estimate the main heat fluxes and energies and some extra parameter-based analyses can be made [17]. The reason to select this type of model is that we looked for a model with low computational needs that permitted us to perform many simulations in a short period of time, i.e., a model that was able to simulate a two-hour cooking process in only a few seconds. In order to simplify the modeling process, the model was built following the method and recommendations given in the previously cited paper. For your information, the connection between lumped capacitance models and heat transfer physical phenomena is also explained in the same reference.

When using a lumped capacitance structure, a system is modeled as a set of thermal capacitors interconnected with each other by means of thermal resistances. Additionally, external temperatures or heat fluxes may exist as boundary conditions. Considering a general system whose only external temperature is the ambient temperature T_{amb}, each lump i of the model (Fig. 3) has an equation of the following form:

$$C_i \frac{dT_i}{dt} = \sum_{\substack{j=1 \\ j \neq i}}^{n} \frac{1}{R_{j,i}}(T_j - T_i) + \frac{1}{R_{amb,i}}(T_{amb} - T_i) + \dot{Q}_i, \tag{1}$$

4

Table 1. Components of the actual system and linked lumps in the model. Note that the load has been modeled as a two-layer object.

Lump	Actual component	Number of thermocouples
1	Top outer heater	4
2	Top inner heater	4
3	Ring heater	4
4	Bottom heater	4
5	Cavity metal sheets	40
6	External metal sheets	45
7	Load (external layer)	2 (B1, B2)*
8	Load (internal layer)	2 (A1, A2)*

*See Fig. 2

where n is the order of the model, C_i the thermal capacitance of lump i, $R_{j,i}$ and $R_{amb,i}$ the thermal resistances between node i and, respectively, node j and the ambient, T_i the temperature of node i and $\dot{Q}_i$ the boundary heat flux that directly flows into capacitance C_i.

The selection of order n should be a trade-off between the precision of the model and its complexity. In our application, temperature records of Set B were analyzed by means of time series clustering methods and we found that they could be separated in eight different sets which, in addition, corresponded almost exactly to specific components or zones of the oven or the thermal load. This analysis led us to set a model order of $n = 8$. In other words, this means that we modeled the system as a set of 8 thermal lumps. If specific components of the system such as, e.g., the thermostat, were of particular interest, additional equations can be included to model these elements by using the same procedure that we present in the paper. The link between the actual components of the system and the lumps of the model, as well as the number of thermocouples involved, are presented in Table 1.

The general expression for all the lumps of the model (1) can now be modified to the specific characteristics of each one. First of all, the temperature registered by the thermocouple placed in the middle of the laboratory is assigned as ambient temperature T_{amb}. Although ambient temperature has a considerable influence on the energy losses of the oven, it affects directly only on the external components of the system. Consequently, only the connection between the ambient and lump 6 makes sense and all the others may be considered negligible. Regarding the model, this is achieved by considering $R_{amb,i} = \infty$, $\forall\, i \neq 6$.

Moisture evaporation during a cooking process requires a significant amount of energy and should not be ignored when building a model of an oven. Let $\dot{Q}_{ev}$ be the heat flux absorbed by the evaporation process. Then, as evaporation drains energy from the surface of the load, $\dot{Q}_7 = -\dot{Q}_{ev}$. Note that surface evaporation heat flux $\dot{Q}_{ev}$ might be nearly impossible to measure. However, it can be calculated if water evaporation rate $\dot{m}_{ev}$ is known,
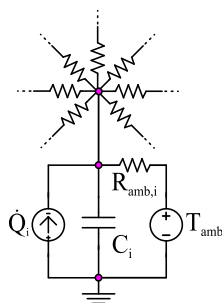

Fig. 3. Schematic of a general node i in a lumped capacitance model.

5

$$\dot{Q}_{ev} = \Delta H_{vap} \cdot \dot{m}_{ev}, \tag{2}$$

being ΔH_{vap} the enthalpy of vaporization of water in energy per unit mass. Mass evaporation rate $\dot{m}_{ev}$ may then be obtained either from mass measurements or estimated by means of the experimental expression developed in this research and presented in section 3.2.

Hence, by means of Eq. (2), the phenomenon of evaporative cooling and the loss of mass of the brick have been incorporated to the model. Since water evaporation also modifies the humidity of the air inside the oven, its influence over the oven parameters may have been taken into account too. However, like most of the convection ovens in the market, the unit used in this research features a vapor outlet that prevents from strong changes in the air humidity during the cooking. According to this and considering that we looked for a model with low computational needs, humidity dependence of the model parameters has been assumed negligible. Note that this assumption, which may be adopted for convection ovens like the one investigated in the paper, may not be correct for steam ovens where humidity variation is considerably higher.

The power supplied by each one of the heating elements acts as an independent input of the oven. Let $\dot{Q}_{TOH}$, $\dot{Q}_{TIH}$, $\dot{Q}_{RH}$ and $\dot{Q}_{BH}$ be the heat fluxes generated, respectively, by the top outer, top inner, ring and bottom heating elements. Then, given that each of these elements is linked to a specific lump of the model (Table 1), we set $\dot{Q}_1 = \dot{Q}_{TOH}$, $\dot{Q}_2 = \dot{Q}_{TIH}$, $\dot{Q}_3 = \dot{Q}_{RH}$ and $\dot{Q}_4 = \dot{Q}_{BH}$. Finally, lumps 5, 6 and 8, which are respectively linked to the oven cavity, the external metallic components and the interior of the thermal load, are not directly subjected to any heat flux, i.e., $\dot{Q}_5 = \dot{Q}_6 = \dot{Q}_8 = 0$.

By substituting the previous expressions and developing (1) for $i = 1, ..., 8$, the system of differential equations of the model is obtained.

$$C_1 \frac{dT_1}{dt} = \sum_{j=2}^{8} \frac{1}{R_{j,1}} (T_j - T_1) + \dot{Q}_{TOH}, \tag{3}$$

$$C_2 \frac{dT_2}{dt} = \sum_{\substack{j=1 \\ j \neq 2}}^{8} \frac{1}{R_{j,2}} (T_j - T_2) + \dot{Q}_{TIH}, \tag{4}$$

$$C_3 \frac{dT_3}{dt} = \sum_{\substack{j=1 \\ j \neq 3}}^{8} \frac{1}{R_{j,3}} (T_j - T_3) + \dot{Q}_{RH}, \tag{5}$$

$$C_4 \frac{dT_4}{dt} = \sum_{\substack{j=1 \\ j \neq 4}}^{8} \frac{1}{R_{j,4}} (T_j - T_4) + \dot{Q}_{BH}, \tag{6}$$

$$C_5 \frac{dT_5}{dt} = \sum_{\substack{j=1 \\ j \neq 5}}^{8} \frac{1}{R_{j,5}} (T_j - T_5), \tag{7}$$

$$C_6 \frac{dT_6}{dt} = \sum_{\substack{j=1 \\ j \neq 6}}^{8} \frac{1}{R_{j,6}} (T_j - T_6) + \frac{1}{R_{amb,6}} (T_{amb} - T_6), \tag{8}$$

$$C_7 \frac{dT_7}{dt} = \sum_{\substack{j=1 \\ j \neq 7}}^{8} \frac{1}{R_{j,7}} (T_j - T_7) - \Delta H_{vap} \cdot \dot{m}_{ev}, \tag{9}$$

$$C_8 \frac{dT_8}{dt} = \sum_{j=1}^{7} \frac{1}{R_{j,8}} (T_j - T_8). \tag{10}$$

Let $\mathbf{u} = (\dot{Q}_{TOH}, \dot{Q}_{TIH}, \dot{Q}_{RH}, \dot{Q}_{BH})^T$ be the input vector of the model and, since T_{amb} and $\dot{m}_{ev}$ are either unknown or non controllable, let $\mathbf{d} = (T_{amb}, \dot{m}_{ev})^T$ be a disturbance vector. If temperatures T_1 to T_8 are selected as state variables, i.e., $\mathbf{x} = (T_1, T_2, T_3, T_4, T_5, T_6, T_7, T_8)^T$, a minimal state space realization of the form $\dot{\mathbf{x}} = A \cdot \mathbf{x} + B \cdot \mathbf{u} + B_d \cdot \mathbf{d}$ may be obtained, being A the 8-by-8 state matrix, B the 8-by-4 input matrix and B_d the 8-by-2 disturbance matrix. Although a black-box state space model of the same size would have 112 independent parameters, our model is internally dependent on only 37 unknown parameters: 8 thermal capacitances and 29 thermal resistances (note that $R_{j,i} = R_{i,j}, \forall j, i$). The difference can be interpreted as restrictions included to give physical sense to the model.

3.2. Water evaporation estimation

Water evaporation in cooking processes like roasting or baking is a non negligible phenomenon that should be considered when building a complete thermal model. If ignored, important effects such as food drying or evaporative cooling would not be taken into account. Inside an oven, water evaporation takes place in the surface of the food and its rate is usually assumed to be proportional to the relative humidity difference that exists between the external layer of the product and the air that surrounds it. Nevertheless, this relationship is only valid at constant conditions since the process is strongly dependent on the air velocity, the temperature of both the food and the air and the moisture transport inside the product. This complex dynamics makes the process very difficult to model, at least in a comprehensive manner. For that reason, the following experimental and nonlinear expression is proposed to estimate the water evaporation rate $\dot{m}_{ev}$ of the thermal load:

$$\dot{m}_{ev} = -\frac{dm_w}{dt} = a_0 + a_1 \cdot T_{load}(t) + a_2 \cdot T_{oven}(t) + a_3 \cdot T_{load}(t) \cdot T_{oven}(t), \tag{11}$$

where m_w is the water mass in the load, T_{load} and T_{oven} are temperatures of the thermal load and the oven, respectively, and a_0, a_1, a_2 and a_3 are constants to determine. The minus sign indicates that the water evaporation rate $\dot{m}_{ev}$ is positive when the water mass m_w is decreasing. Note that, for constant oven temperature, $T_{oven}(t) = T_{oven,CST}$, (11) becomes a linear relationship between $\dot{m}_{ev}$ and T_{load},

$$\dot{m}_{ev} = -\frac{dm_w}{dt} = b_0 + b_1 \cdot T_{load}(t), \tag{12}$$

where b_0 and b_1 depend linearly on the constant oven temperature $T_{oven,CST}$.

$$b_0 = a_0 + a_2 \cdot T_{oven,CST}, \tag{13}$$
$$b_1 = a_1 + a_3 \cdot T_{oven,CST}. \tag{14}$$

If the experiment is a classical baking or roasting process, where the oven temperature remains almost constant during a long time, (12) provides simpler calculations and may be accurate enough to estimate the water evaporation rate. In addition, note that (11) also becomes a linear expression for constant load temperature. However, due to the much slower dynamics of the thermal load respect to the oven, this case is extremely rare in practice.

In the experimental tests carried out in this research, the oven had a transient response because of the initial conditions that prevents from using (12). The water evaporation rate of the thermal load was then adjusted to the complete expression (11), using data from the tests of Set A. The average temperature of thermocouples A1 and A2 (Fig. 1) was selected as load temperature T_{load}, and the average temperature of the 40 thermocouples distributed in the oven cavity (Table 1) was used as oven temperature T_{oven}. In order to directly use mass measurements and avoid problems in differentiating signals which were likely to be noisy, (11) was transformed to integral form,

$$m_{ev}(t) = m_{w,t0} - m_w(t) = a_0 \cdot f_1(t) + a_1 \cdot f_2(t) + a_2 \cdot f_3(t) + a_3 \cdot f_4(t), \tag{15}$$

where m_{ev} is the evaporated water mass, $m_{w,t0}$ is the initial water mass in the load and f_1, f_2, f_3 and f_4 are integral terms that can be calculated from T_{load} and T_{oven}.

7

$$f_1(t) = t, \tag{16}$$

$$f_2(t) = \int_0^t T_{load}(\tau) \cdot d\tau, \tag{17}$$

$$f_3(t) = \int_0^t T_{oven}(\tau) \cdot d\tau, \tag{18}$$

$$f_4(t) = \int_0^t T_{load}(\tau) \cdot T_{oven}(\tau) \cdot d\tau. \tag{19}$$

Supposing that there is no thermal decomposition of the matter or it is insignificant, every variation in the load will be due to water evaporation,

$$m_{load,t0} - m_{load}(t) = m_{w,t0} - m_w(t), \tag{20}$$

where $m_{load,t0}$ and m_{load} are the initial and the time-dependent load mass, respectively. Finally, by substituting (20) in (15),

$$m_{ev}(t) = m_{load,t0} - m_{load}(t) = a_0 \cdot f_1(t) + a_1 \cdot f_2(t) + a_2 \cdot f_3(t) + a_3 \cdot f_4(t), \tag{21}$$

equation that can be directly adjusted to the data by using the least squares method. Considering that water evaporation is greatly influenced by air velocity, two different fittings were made, each corresponding to one of the possible fan states. To this end, Set A was divided in two subsets: Subset A.1, which included the tests with the fan turned off, and Subset A.2, with the remaining tests. Each subset provided a parameter set $[a_0, a_1, a_2, a_3]$ which may be used to estimate the water evaporation rate of the brick, either in the case of activated or deactivated fan. The results of both fittings are shown in Table 2 and Figs. 4 and 5. It must be noted that Eq. (11) only depends on the fan state and the temperatures of the cavity and the internal layer of the load, which are respectively given in the model by T_5 and T_8. In this way, heat flux $\dot{Q}_{ev}$ may be estimated for different thermal dynamics without need of additional mass measurements.

Table 2. Water evaporation estimation. Main results of the adjustment to Eq. (21).

Subset	Fan state	$RMSE$ (g)	$RMSE/(m_{max} - m_{min})$
A.1	Off	2.86	1.84%
A.2	On	6.78	2.64%

$RMSE$: Root Mean Square Error

3.3. Identification

The parameters of the lumped model were identified using temperature and power records of Set B. Similarly to the adjustment process of Eq. (21), experimental data were divided in two different subgroups depending on the fan state of each experiment. Initially, it was thought that two parameter sets were necessary, one for fan activated and another for fan deactivated. Nevertheless, both sets should have been interrelated, since the fan state only changes the convective conditions and they are not related to thermal capacitances, only to resistances. As a result, instead of two independent parameter sets, only a extended one was determined. This set, which will be called θ, includes 66 parameters: 8 thermal capacitances, which are the same independently of the fan state, and 58 thermal resistances, 29 for fan activated and 29 for fan deactivated. Temperature records were processed through Eqs. (2) and (11) obtaining an estimation of the power absorbed by surface evaporation, $\dot{Q}_{ev}$, for use in the identification. Direct measurements of the
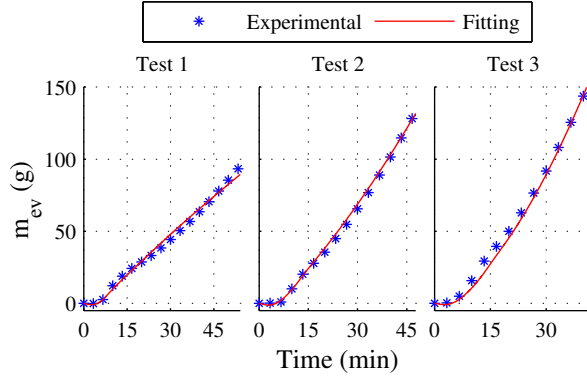
Fig. 4. Experimental data from Subset A.1 and fitting to Eq. (21). Subset A.1 includes 3 tests with the fan turned off. To simplify the representation, only one of every hundred experimental points is represented.
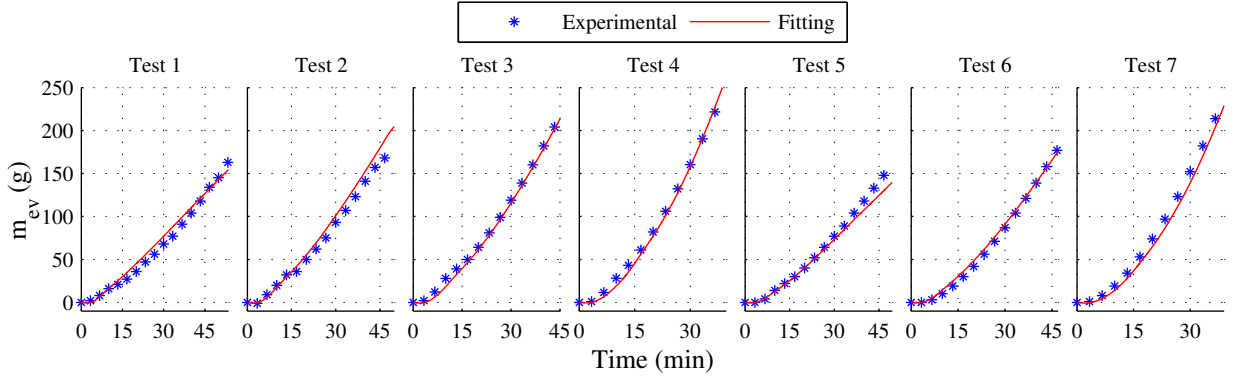

Fig. 5. Experimental data from Subset A.2 and fitting to Eq. (21). Subset A.2 includes 7 tests with the fan turned on. To simplify the representation, only one of every hundred experimental points is represented.

brick mass could not be utilized because of the high presence of noise. The values of the parameters were determined by minimizing the following weighted error function:

$$E(\theta) = \sum_{i=1}^{8} w_i \cdot e_i(\theta),$$ (22)

$$e_i(\theta) = \frac{\sqrt{\sum_{k=1}^{m}(T_i(k) - \hat{T}_i(k))^2}}{max(T_i) - min(T_i)},$$ (23)

where $T_i(k)$ and $\hat{T}_i(k)$ are the registered and the given by the model temperatures of lump i at time k, m is the total number of samples and w_i is the weight given to error e_i. Note that error function $E(\theta)$ is dimensionless, since every temperature error $e_i(\theta)$ is scaled to $max(T_i) - min(T_i)$. Average temperatures of the thermocouples linked to each lump (Table 1) were used as temperatures $T_i(k)$. Since negative resistances or capacitances do not make physical sense, restrictions were included to assure that they were positive. The Global Search algorithm included in MATLAB Global Optimization Toolbox was used to minimize $E(\theta)$, obtaining the optimum parameter set θ^*. The weights given to temperatures and the obtained identification errors are presented in Table 3. Fig. 6 shows both experimental and simulated cavity temperature (T_5) at the end of the identification process.

The identification results showed that the model fitted accurately to the temperature dynamics of both oven and load, but at this point several questions raised: Was there a direct relationship between the com-

Table 3. Components of the actual system and corresponding weights and identification errors. Temperatures of the internal cavity and the load were considered more important and received a higher weight.

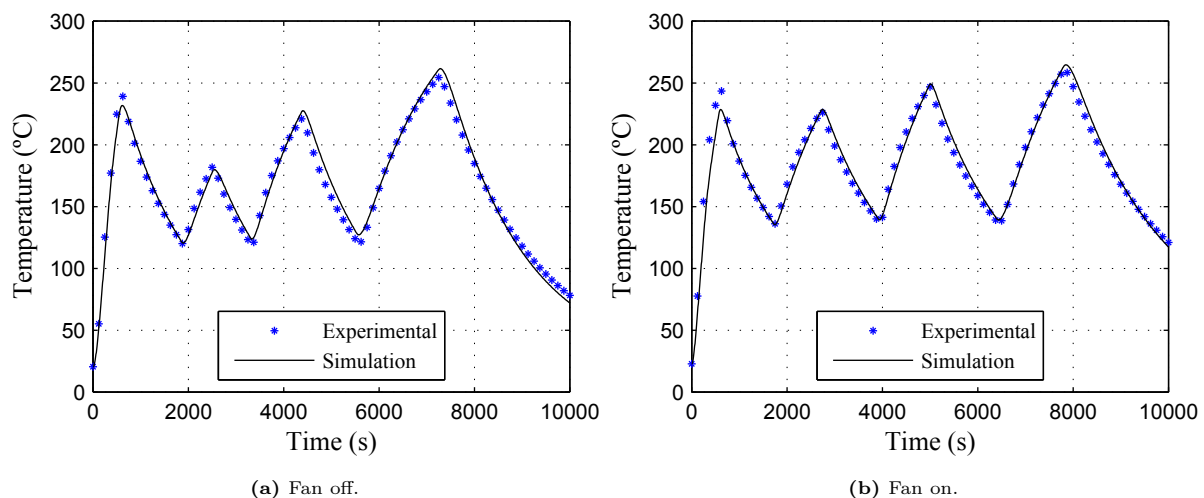| Lump	Actual component	Weight (w_i)	Error ($e_i(\theta^*)$)
1	Top outer heater	0.075	0.029
2	Top inner heater	0.075	0.034
3	Ring heater	0.075	0.029
4	Bottom heater	0.075	0.046
5	Cavity metal sheets	0.375	0.030
6	External metal sheets	0.075	0.035
7	Load (external layer)	0.125	0.029
8	Load (internal layer)	0.125	0.027

(a) Fan off.

(b) Fan on.

Fig. 6. Experimental (average of 40 thermocouples) and simulated cavity temperature (T_5 in the model) after the identification process. Only one of every twenty-five experimental points is represented.

ponents of the real system and the parameters of the model, or was the parameter set only a combination of numbers that provides a good estimation of temperatures? Could we extract conclusions from the identified values of thermal capacitances and resistances? Apart from temperatures, were also the heat fluxes and thermal energies given by the model an estimation of the real ones in the actual system? In short, did the model and its parameters really have a physical sense?

All this questions were directly connected to model identifiability. If achieved, this property assures that there exists only one global parameter set for a model so that it is unequivocally related to the real system. Identifiability demonstration of physically based models is however a hard problem because of the likely arbitrary and non-linear parametrization. To solve the problem, the differential-algebraic method based on Ritt's algorithm [18] and proposed by Ljung and Glad in [19] for arbitrary parametrized models was utilized in this research.

Our model, even though it was linear in variables, presented non-linearity in parameters because of the use of resistances, which were dividing temperature differences. This non-linearity, which highly increases the time complexity of the method, was easily solved by substituting resistances by conductances. In this way, every node equation of the model, (1), was transformed into

$$C_i \frac{dT_i}{dt} = \sum_{\substack{j=1 \\ j \neq i}}^{n} G_{j,i}(T_j - T_i) + G_{amb,i}(T_{amb} - T_i) + \dot{Q}_i, \tag{24}$$

10

where $G_{j,i}$ and $G_{amb,i}$ are the thermal conductances between nodes i and, respectively, node j and the ambient. A simplified version of the algorithm, adapted to our model, was implemented in MATLAB using the Symbolic Math Toolbox. Since the modified model is linear both in variables and parameters, the algorithm only required the application of Gaussian eliminations and Ritt's pseudodivisions to obtain the characteristic set of model equations. The final expressions are long enough to take up hundreds of pages, but they definitely proved that our model was globally identifiable. If interested, a copy of the results can be obtained upon request to the authors.

4. Energy analysis. Results and discussion

Once model identifiability is proved, the developed model can be used to carry out simulations and extract useful information from both oven and thermal load. Two different one-hour cooking processes have been simulated to analyze the energy behavior of the system. The first one corresponds to a convective cooking method such as bread baking, therefore the oven has been heated by using only the ring heating element in combination with the fan. On the other hand, the second test has simulated a mostly radiative process like meat roasting, so only the top and bottom heating elements have been used and the fan has remained turned off. More cooking processes have been simulated, but these two were considered the most representative. To properly compare the results, the set point oven temperature in both simulations has been established to 200ºC and the initial state has been the same as in the experimental tests (section 2.2).

If only the total energy consumption was studied, not too much information would be obtained. In fact, both processes use approximately the same amount of energy ($\approx$1200Wh) to keep the cavity at the set temperature during one hour. This information could have even been measured in the real oven, but our model has permitted a deeper analysis. Fig. 7 shows how energy is distributed among the oven components, the load and the ambient at the end of the preheating stage. As expected, energy in this phase has been mainly used in heating up the cavity, so convective and radiative methods are energetically not very different at this point. It is only remarkable that the energy stored in the heating elements is nearly twice in the radiative method than in the convective one, principally because three elements have been used instead of a single one.
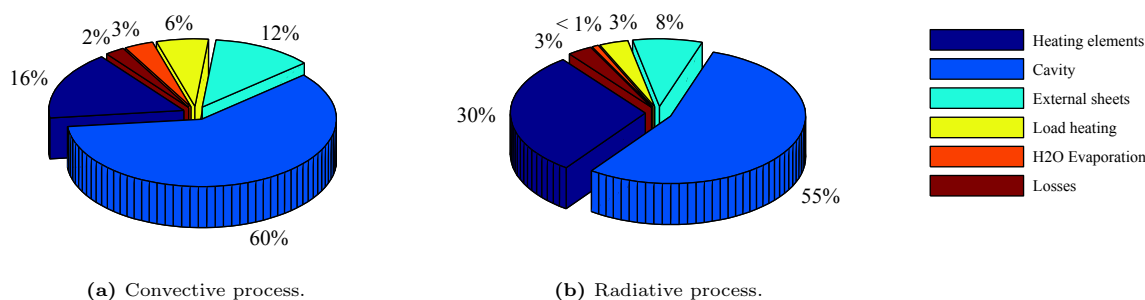

(a) Convective process. **(b)** Radiative process.

Fig. 7. Distribution of the energy supplied to the oven at the end of preheating stage.

Energy distributions have nevertheless changed considerably at the end of the simulations (Fig. 8). Heat has been more evenly distributed in the convective process and the load has received a larger amount of energy, about 13% compared to 11% in the radiative one. However, this operating mode has also caused a high increase in water evaporation (20% of the energy compared to 8%). Note that these properties precisely explain the main uses of the methods: in bread or cake baking, where an even heat distribution and a considerable water evaporation are needed, convective heating is preferred; in contrast, radiative methods are more appropriate for meat or fish roasting, where water evaporation has to be minimized in order to keep the food juicy and succulent.

It is also noteworthy that energy losses in the radiative simulation have been much higher than in the convective one, mainly in stationary state. Although no obvious reasons seem to explain this behavior, an
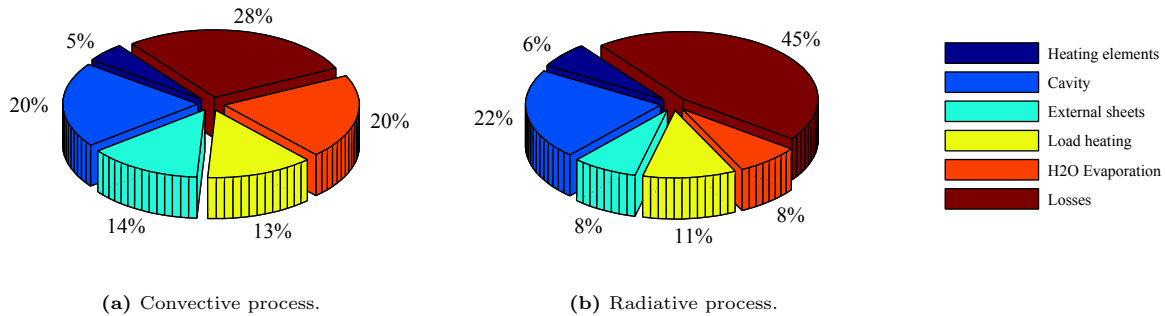
(a) Convective process.   **(b)** Radiative process.

Fig. 8. Distribution of the energy supplied to the oven at the end of experiments.

analysis of the model parameters and a subsequent visual inspection of the real oven has shown that it is related to two different causes. Firstly, that the insulation of the bottom part is worse than in the rest of the oven, so efficiency is reduced when the bottom heating element is utilized. And secondly, that the fan operation causes the heat generated in the ring heating element to flow into the cavity so less energy is lost through the rear side. In this regard, the energy analysis provided by the model has been the key to detect these problems.

An even more comprehensive analysis can be obtained from time-dependent graphs like Figs. 9 and 10, where supplied power and energy consumption have been respectively represented, both divided in their corresponding time-dependent uses. These graphs show, for example, that the oven is still being heated after the end of the preheating stage because the external sheets have not reached their stationary temperature. It is also significant how water evaporation dynamics is influenced by fan operation: while water is evaporated almost immediately after the beginning of the convective test, in the radiative one the evaporation requires a higher temperature to start. All this knowledge of the system is essential for designing new and better algorithms that may be able, for example, to control not only the cavity temperature, but also the water evaporation rate or the temperature of the food itself without need of additional sensors. Note that the simultaneous control of these variables is precisely the key for obtaining optimum cooking results. Furthermore, information of energy stored in the oven components may be used, for example, to switch off the system before the end of the cooking process so that the food is eventually cooked by using only the remaining energy. In this way, energy consumption may be reduced and the appliance would then become more energy-efficient.

Finally, it must also be noted that model parameters can be used to perform additional analyses because of their physical meaning. In this regard, it has been studied the possibility of removing the top inner heating element so that all the power from the top side is supplied by an unique double-power heater. Capacitance C_{TIH} has been consequently made zero in the model and new simulations have been carried out. The results state that energy consumption would be reduced by 0.9% in the one-hour convective process and by 1.3% in the radiative one, mainly because the mass to be heated would be lower. Similar model changes may also be made to evaluate the system performance under several conditions: the use of a new cavity material of a different specific heat, a load of double mass, a thicker insulation, etc.

5. Conclusions

A new heat and mass transfer model of an electric oven which differentiates the components of the appliance and the load located inside has been developed and presented. The model, which is based on a lumped structure and has been identified by using temperature, mass and power records from experimental tests, is able to estimate several variables of the system such as temperatures, heat fluxes or stored energies.

An experimental expression to estimate the water evaporation of the thermal load has been also included in the model so that the effect of evaporation is considered and evaluated. In spite of not being based on
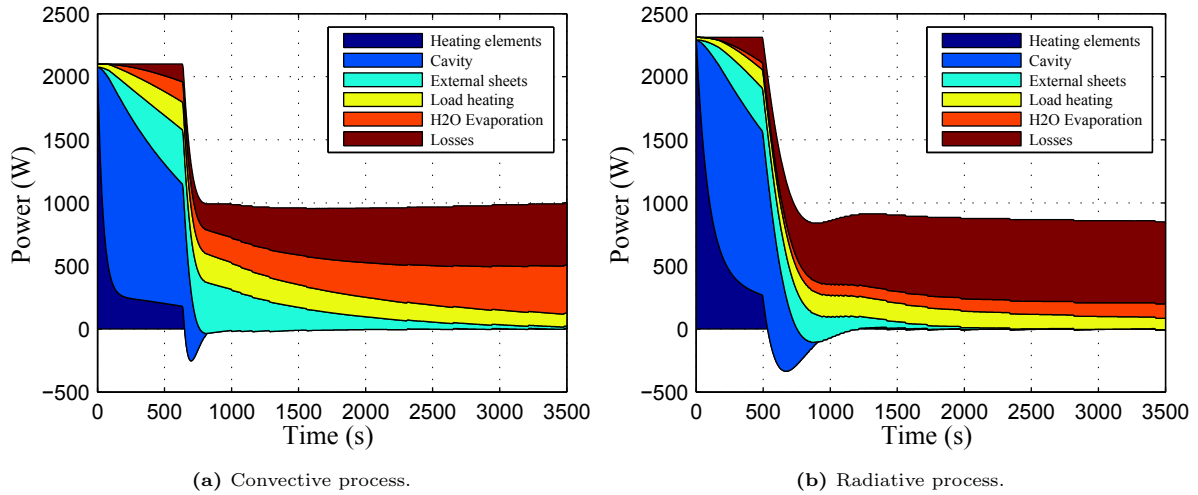
(a) Convective process.

(b) Radiative process.

Fig. 9. Time-dependent power consumption.

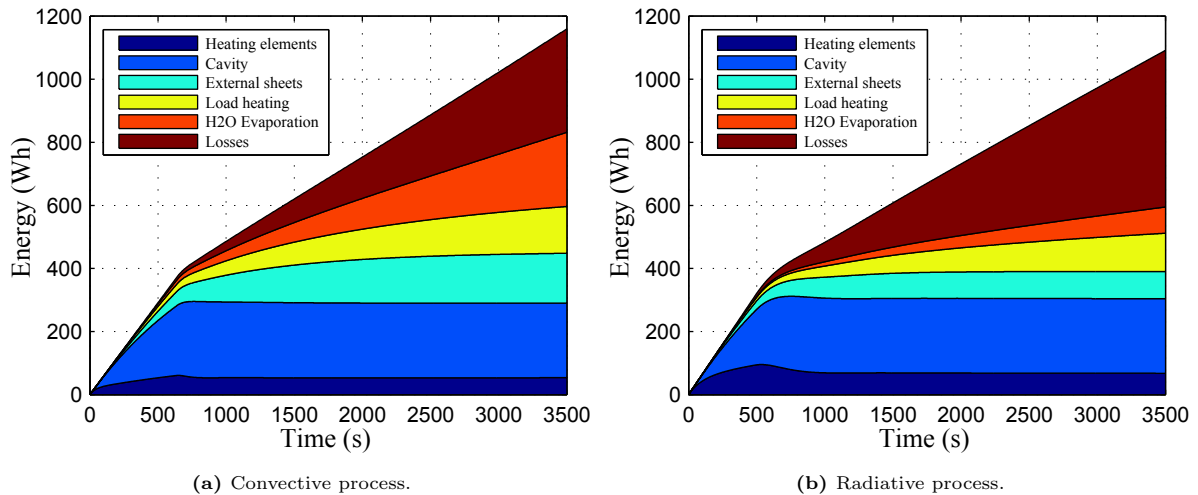**(a)** Convective process.

(b) Radiative process.

Fig. 10. Time-dependent energy consumption.

actual physical phenomena, this expression has been able to provide a great estimation of the evaporation rate under diverse heating conditions without need of complex calculations.

Since model parameters are directly related to the actual components of the system, the presented model is highly versatile and can be easily modified to analyze the oven performance under various conditions. In addition, contrary to FEM or CFD models, our low order structure achieves satisfactory results in very fast calculations. In this sense, the model is well suited to iterative simulation processes involving some type of optimization. It may be used, e.g., to design novel temperature controllers or estimators that might overcome the state-of-the-art ones in terms of energy efficiency and cooking results.

Acknowledgment

References

[1] E. Purlis, "Baking process design based on modelling and simulation: Towards optimization of bread baking," *Food control*, vol. 27, no. 1, pp. 45–52, 2012.

[2] K. Unklesbay, A. Boza-Chacon, and N. Unklesbay, "Air temperature transfer function of a convection oven," *Food Control*, vol. 8, no. 1, pp. 39–43, 1997.

[3] V. Ryckaert, J. Claes, and J. Van Impe, "Model-based temperature control in ovens," *Journal of food engineering*, vol. 39, no. 1, pp. 47–58, 1999.

[4] I. Sanchez, J. R. Banga, and A. A. Alonso, "Temperature control in microwave combination ovens," *Journal of Food Engineering*, vol. 46, no. 1, pp. 21–29, 2000.

[5] P. Mirade, J. Daudin, F. Ducept, G. Trystram, and J. Clement, "Characterization and cfd modelling of air temperature and velocity profiles in an industrial biscuit baking tunnel oven," *Food research international*, vol. 37, no. 10, pp. 1031–1039, 2004.

[6] J. P. Ploteau, V. Nicolas, and P. Glouannec, "Numerical and experimental characterization of a batch bread baking oven," *Applied Thermal Engineering*, vol. 48, pp. 289–295, 2012.

[7] Z. Khatir, J. Paton, H. Thompson, N. Kapur, V. Toropov, M. Lawes, and D. Kirk, "Computational fluid dynamics (cfd) investigation of air flow and temperature distribution in a small scale bread-baking oven," *Applied Energy*, vol. 89, no. 1, pp. 89–96, 2012.

[8] M. Boulet, B. Marcos, M. Dostie, and C. Moresoli, "Cfd modeling of heat transfer and flow field in a bakery pilot oven," *Journal of Food Engineering*, vol. 97, no. 3, pp. 393–402, 2010.

[9] S.-Y. Wong, W. Zhou, and J. Hua, "Cfd modeling of an industrial continuous bread-baking process involving u-movement," *Journal of Food Engineering*, vol. 78, no. 3, pp. 888–896, 2007.

[10] J. P. Abraham and E. M. Sparrow, "A simple model and validating experiments for predicting the heat transfer to a load situated in an electrically heated oven," *Journal of food engineering*, vol. 62, no. 4, pp. 409–415, 2004.

[11] M. Sakin, F. Kaymak-Ertekin, and C. Ilicali, "Simultaneous heat and mass transfer simulation applied to convective oven cup cake baking," *Journal of food engineering*, vol. 83, no. 3, pp. 463–474, 2007.

[12] M. Sakin-Yilmazer, F. Kaymak-Ertekin, and C. Ilicali, "Modeling of simultaneous heat and mass transfer during convective oven ring cake baking," *Journal of Food Engineering*, vol. 111, no. 2, pp. 289–298, 2012.

[13] A. H. Feyissa, K. V. Gernaey, and J. Adler-Nissen, "3d modelling of coupled mass and heat transfer of a convection-oven roasting process," *Meat science*, vol. 93, no. 4, pp. 810–820, 2013.

[14] A. P. Ramallo-González, M. E. Eames, and D. a. Coley, "Lumped parameter models for building thermal modelling: An analytic approach to simplifying complex multi-layered constructions," *Energy and Buildings*, vol. 60, pp. 174–184, 2013.

[15] S. Royer, S. Thil, T. Talbert, and M. Polit, "A procedure for modeling buildings and their thermal zones using co-simulation and system identification," *Energy and Buildings*, vol. 78, pp. 231–237, 2014.

[16] C. Underwood, "An improved lumped parameter method for building thermal modelling," *Energy and Buildings*, vol. 79, pp. 191–201, 2014.

[17] E. Ramírez-Laboreo, C. Sagüés, and S. Llorente, "Thermal modeling, analysis and control using an electrical analogy," in *Control & Automation, 2014. MED'14. Mediterranean Conference on.* IEEE, 2014, pp. 505–510.

[18] J. F. Ritt, *Differential algebra.* American Mathematical Soc., 1966, vol. 33.

[19] L. Ljung and T. Glad, "On global identifiability for arbitrary model parametrizations," *Automatica*, vol. 30, no. 2, pp. 265 – 276, 1994.